

Asymmetric Propulsion: Thrust and Maneuverability from a Single Degree of Freedom

Jeff Kaeli, Robin Littlefield, Fred Jaffre

Ocean Systems Laboratory, Applied Ocean Physics and Engineering Department

Woods Hole Oceanographic Institution (WHOI)

Woods Hole, MA, USA

{jkaeli, rlittlefield, fjaffre}@who.edu

Abstract—We present ongoing work on an asymmetric propulsion system capable of simultaneously generating both forward thrust as well as a turning moment from a single degree of freedom. By a single degree of freedom, we mean a single rotating propeller powered by a single motor, absent of additional mechanisms such as fins or actuators. This is accomplished by actively controlling the instantaneous rotational velocity of a propeller whose blades are distributed asymmetrically around the axis of rotation. Due to the nonlinear relationship between velocity and thrust, the mean thrust vector produced over the course of a rotation will be shifted away from the axis of rotation. This shift induces a turning moment whose strength and orientation can be controlled to provide lateral maneuverability in addition to forward or reverse thrust. We demonstrate how this can be used to control and maneuver an underwater robot and discuss its advantages and applications to autonomous underwater vehicle (AUV) design and operation.

Index Terms—propulsion, autonomous underwater vehicle

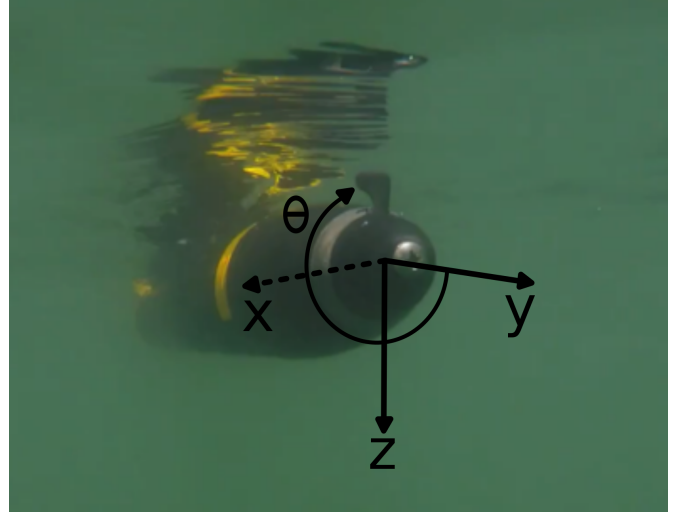


Fig. 1. An asymmetric propulsion system utilizing a single-bladed propeller. The coordinate system is shown with the x -axis forward, z -axis downward, and blade orientation θ measured clockwise from the starboard y -axis.

I. INTRODUCTION

The form factors and propulsion systems employed by unmanned underwater robots are largely driven by the tasks they perform. Remotely operated vehicles (ROVs) receive power and control commands from an operator by means of a tether and are often tasked with performing fine scale manipulation. They must be capable of holding station over areas of interest, and they accomplish this with multiple thrusters capable of providing instantaneous thrust in any direction. Autonomous underwater vehicles (AUVs), by contrast, are free-swimming, streamlined, and are more often utilized for surveying broad areas of the seafloor and transiting long distances. AUVs generally rely on a propeller to provide thrust and additional control surfaces or fins to provide lateral maneuverability. However, these control surfaces require flow over them to remain effective, so the AUV must maintain some minimum forward speed to maneuver. AUVs specifically designed for low-speed maneuverability have multiple propellers and perform tasks such as building photomosaics of the seafloor that require very stable platforms and large overlap between successive images frames.

All of the aforementioned propulsion systems rely on propellers with multiple blades that are symmetrically distributed around the axis of rotation. The propeller rotates at a constant velocity, and the resulting thrust is proportional to the square of this velocity. This thrust vector acts along the axis of

the propeller shaft because of the symmetry in the blade distribution. In contrast, an asymmetric propulsion system can produce an average thrust vector that is off-axis of the propeller shaft and is thus able to provide both forward thrust as well as a turning moment for the vehicle [1]. The system is termed “asymmetric” because the propeller blades are asymmetrically distributed around the axis of rotation. In the case of the system presented in this paper, the asymmetry arises from the use of a propeller with a single blade as shown in Figure 1. However, other manifestations using multiple asymmetrically distributed blades are possible as well.

This technology confers several advantages over traditional vehicle control systems. It is mechanically less complex, requiring fewer components, moving parts, and through-hull penetrations, resulting in fewer failure modes and subsequently a lower overall system failure rate. It also enables a smaller overall physical footprint, making it an attractive choice for smaller AUVs. Furthermore, the use of actuated fins or other control surfaces creates additional drag. The elimination of these drag-generating features improves both speed and endurance of the vehicle which is critical in a system where available energy is limited [2]. Furthermore, fins and rudders

require flow over their control surfaces to be effective. An asymmetric propulsion system can maintain maneuverability without the requirement of forward motion to generate flow over control surfaces. Operating at low speeds reduces the power consumption of the propulsion system, increasing the mission endurance and the linear coverage of the seafloor for a given power budget [3].

In this paper, we first formulate a mathematical model of an asymmetric propulsion system, derive various control parameters, and discuss our implementation using a custom motor controller, thruster, and test platform. We then present preliminary results from in-water tests that demonstrate the ability to maneuver around the surface of a harbor, as well as tank tests that demonstrate an ability to maneuver in place. We conclude with a discussion of the relative merits of this novel propulsion scheme and suggest new kinds of missions its adoption will enable.

II. RELATED WORK

Actively controlling the angle of attack (AOA) of propeller blades throughout their rotation has been extensively studied in the context of helicopters, variable pitch propellers, and Voith-Schneider propellers [4]. Such systems have two or more mechanical degrees of freedom: the propeller shaft, and the mechanism or mechanisms used to control the AOA. Controlling the AOA of a single-bladed propeller has also been proposed [5]. Single-bladed propellers operating at constant speeds have been employed for providing forward thrust to aerial gliders [6] as well as AUVs [7]. In the glider case, the motivation was to enable the propulsion unit to fold into the fuselage for improved aerodynamics when not under power. In the AUV case, the motivation was increased efficiency for a long-endurance vehicle. Recent research supports the claim a single-bladed propeller has the potential to be up to 12% more efficient than traditional multi-bladed propellers [8]. However, the combination of active velocity control and propeller asymmetry to achieve maneuverability from a single degree of freedom is novel to our approach [9].

III. METHODS

A. Formulation

An airfoil generates a lifting force F per span length dr that is proportional to a dimensionless coefficient of force C_F based on its shape, the density of the fluid ρ , the square of the fluid speed U , and its chord length $c(r)$ which varies along the blade.

$$\frac{F}{dr} = C_F \frac{1}{2} \rho U^2 c(r) \quad (1)$$

We can model a single-bladed propeller as an airfoil of span R with an orientation θ relative to the vehicle body rotating at ω radians per second. The instantaneous thrust generated by the propeller can be found by integrating along the length of the blade.

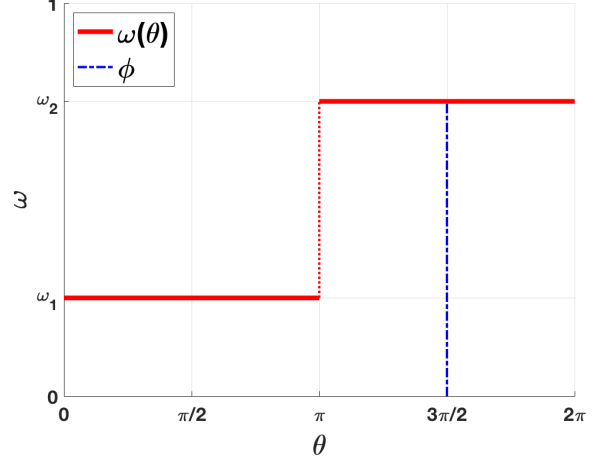


Fig. 2. A simple function dictating angular velocity ω as a function of blade orientation θ . In this example, the orientation of maximum moment $\phi = \frac{3\pi}{2}$ occurs at the center of maximum velocity.

$$F = \int_0^R C_F \frac{1}{2} \rho \underbrace{r^2 \omega^2}_{U^2} c(r) dr \quad (2)$$

If the rotational velocity $\omega(\theta)$ is varied as a periodic function of position, the average force \bar{F} can be found by integrating over one rotation.

$$\begin{aligned} \bar{F} &= \frac{1}{2\pi} \int_0^{2\pi} \int_0^R C_F \frac{1}{2} \rho r^2 \omega(\theta)^2 c(r) dr d\theta \\ &= \frac{\rho}{4\pi} \int_0^R c(r) r^2 \int_0^{2\pi} C_F \omega(\theta)^2 d\theta dr \end{aligned} \quad (3)$$

Similarly, the average moment \bar{M}_ϕ induced by the asymmetric forces can be found by multiplying the force by the moment arm $r \cos(\theta - \phi)$ where ϕ is the steering angle, or the orientation of the maximum moment.

$$\bar{M}_\phi = \frac{\rho}{4\pi} \int_0^R c(r) r^3 \int_0^{2\pi} C_F \omega(\theta)^2 \cos(\theta - \phi) d\theta dr \quad (4)$$

Any number of periodic, or even non-periodic, velocity functions can be explored. For this formulation, however, we define a simple velocity function, illustrated in Figure 2, where the propeller blade rotates at ω_1 for one half of the rotation and at ω_2 for the other half such that $\omega_1 \leq \omega_2$.

$$\omega(\theta) = \begin{cases} \omega_1, & \text{if } 0 \leq \theta \pm 2\pi < \pi \\ \omega_2, & \text{otherwise} \end{cases} \quad (5)$$

We assume that $\omega_1 \in [0, 1]$ and $\omega_2 \in [0, 1]$ are normalized so they are at most 1 radian per second. We also make the simplifying assumption that the chord length varies linearly with the radius $c(r) = ar$.

Based on linear theory for a thin foil at a small angle of attack α , the coefficient of force will have a two components:

one that is proportional to the angle of attack, and one that is a function of the foil shape alone [10].

$$C_F(\alpha) \approx 2\pi\alpha + C_F(\alpha = 0) \quad (6)$$

As the blade velocity varies over each rotation, faster velocities increase the blade's apparent angle of attack while slower velocities decrease the blade's apparent angle of attack. This phenomenon leads to an increase and decrease in force in those sectors, aiding the turning moment and thus aiding maneuverability. We mention it here for completeness, however, we continue our formulation under the assumption that C_F is constant for simplicity. The average force over one full rotation can then be computed.

$$\begin{aligned} \bar{F} &= \frac{C_F \rho a}{4\pi} \int_0^R r^3 dr \left[\int_0^\pi \omega_1^2 d\theta + \int_\pi^{2\pi} \omega_2^2 d\theta \right] \\ &= \frac{C_F \rho a}{16} R^4 (\omega_1^2 + \omega_2^2) \end{aligned} \quad (7)$$

We can also compute the average moment over one full rotation.

$$\begin{aligned} \bar{M}_\phi &= \frac{C_F \rho a}{4\pi} \int_0^R r^4 dr \left[\int_0^\pi \omega_1^2 \cos(\theta - \phi) d\theta \right. \\ &\quad \left. + \int_\pi^{2\pi} \omega_2^2 \cos(\theta - \phi) d\theta \right] \\ &= -\frac{C_F \rho a}{10\pi} R^5 (\omega_2^2 - \omega_1^2) \sin(\phi) \end{aligned} \quad (8)$$

We can determine the orientation of the maximum moment by computing the first and second derivatives with respect to the steering angle ϕ .

$$\frac{d}{d\phi} \bar{M}_\phi = -\frac{C_F \rho a}{10\pi} R^5 (\omega_2^2 - \omega_1^2) \cos(\phi) \quad (9)$$

$$\frac{d^2}{d\phi^2} \bar{M}_\phi = \frac{C_F \rho a}{10\pi} R^5 (\omega_2^2 - \omega_1^2) \sin(\phi) \quad (10)$$

The first derivative will equal 0 at $\phi = \frac{\pi}{2}$ and $\phi = \frac{3\pi}{2}$, and the second derivative will be negative between π and 2π . Thus, the steering angle is $\phi = \frac{3\pi}{2}$, readily seen in Figure 2 as the center of maximum angular velocity. In Figure 1 this would correspond to a downward pitching force causing the platform to dive. In practice, the angular velocity function $\omega(\theta - \phi)$ can take any shape and can be steered to any desired orientation. We can integrate to find the period T of one full rotation.

$$T = \int_0^{2\pi} \frac{1}{\omega(\theta)} d\theta = \frac{\pi}{\omega_1} + \frac{\pi}{\omega_2} \quad (11)$$

Using this relationship, we can also determine the time-averaged angular frequency ω_T over one full rotation.

$$\omega_T = \frac{2\omega_1\omega_2}{\omega_1 + \omega_2} \quad (12)$$

It is apparent that, although the maximum moment occurs when the difference between ω_1 and ω_2 is maximized, there

a practical lower limit to ω_1 as it approaches zero since this will make the period tend towards infinity.

B. Control

Is it useful to implement control parameters that are directly proportional to the forces and moments produced by the system. We define $\mathbf{f} \in [0, 1]$ and $\mathbf{m} \in [0, 1]$ as dimensionless control inputs that are proportional to the thrust and turning moment, respectively.

$$\mathbf{f} = \frac{1}{2}(\omega_1^2 + \omega_2^2) \quad (13)$$

$$\mathbf{m} = \omega_2^2 - \omega_1^2 \quad (14)$$

These relationships are illustrated in Figure 3.

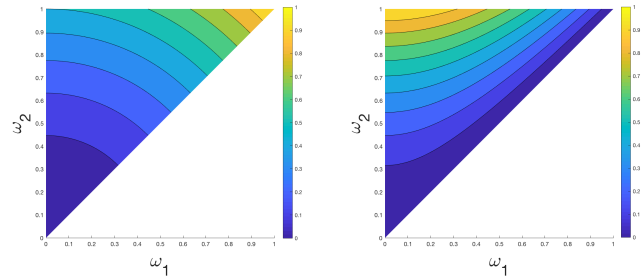


Fig. 3. Force \mathbf{f} (left) and moment \mathbf{m} (right) control parameters as functions of the angular velocities ω_1 and ω_2 .

Note that \mathbf{f} and \mathbf{m} are not defined for $\omega_1 > \omega_2$. The result would be an equal force but with an opposing moment. The same effect can be accomplished with a shift in the steering angle by π .

It is also useful to define rudder $\mathbf{r} \in [-1, 1]$ and elevator control parameters $\mathbf{e} \in [-1, 1]$ that allow control of the heading and pitch similar to conventional propulsion systems.

$$\mathbf{m} = \begin{cases} \sqrt{\mathbf{r}^2 + \mathbf{e}^2}, & \text{if } \mathbf{r}^2 + \mathbf{e}^2 \leq 1 \\ 1, & \text{otherwise} \end{cases} \quad (15)$$

$$\phi = \tan^{-1}\left(\frac{\mathbf{e}}{\mathbf{r}}\right) \quad (16)$$

These relationships are illustrated in Figure 4.

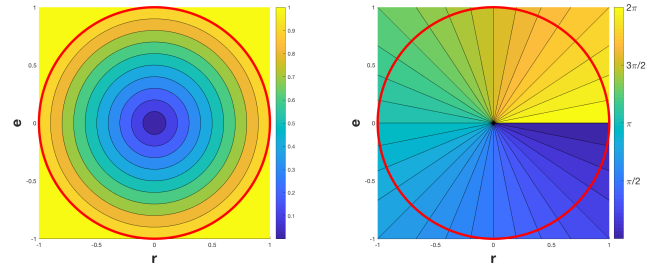


Fig. 4. Steering moment magnitude \mathbf{m} (left) and angle ϕ (right) as functions of the rudder \mathbf{r} and elevator \mathbf{e} control parameters. The red circle corresponds to the region outside of which the magnitudes is restricted to a value of 1.

Magnitudes greater than 1, for instance when both the rudder and elevator are commanded to their full extents, are restricted to a value of 1. The angular velocities can then be determined as a function of these control parameters.

$$\omega_1 = \begin{cases} \sqrt{f - \frac{m}{2}}, & \text{if } f \geq \frac{m}{2} \\ 0, & \text{otherwise} \end{cases} \quad (17)$$

$$\omega_2 = \begin{cases} \sqrt{f + \frac{m}{2}}, & \text{if } f + \frac{m}{2} \leq 1 \\ 1, & \text{otherwise} \end{cases} \quad (18)$$

These relationships are illustrated in Figure 5.

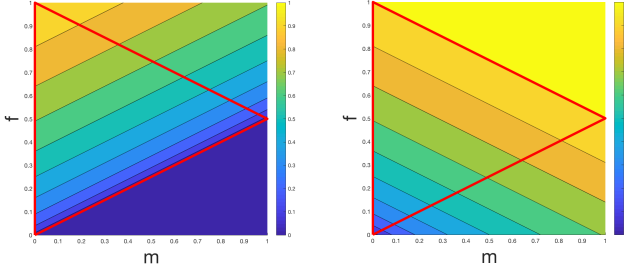


Fig. 5. Angular velocities ω_1 (left) and ω_2 (right) as functions of the force f and moment m control parameters. The red line corresponds to the region outside of which the angular velocities are restricted.

For regions outside the red triangle, the resulting forces and moments will be clamped to their nearest values on the edge of the triangle. This is illustrated in Figure 6.

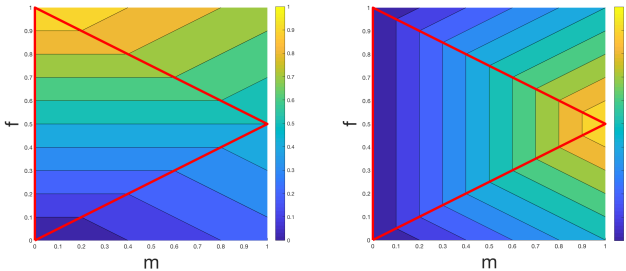


Fig. 6. Resulting proportional force f (left) and moment m (right) as functions of the input force f and moment m control parameters. The red line corresponds to the region outside of which the angular velocities are restricted.

Intuitively, this occurs because asymmetric propulsion requires variations in angular velocity to affect a turning moment. When the velocities are near their maximum or minimum values, there is less freedom for them to vary.

C. Implementation

A motor controller board was custom designed to control the speed of a brushless DC motor through each revolution with a 0.1° resolution at maximum of 3000 RPM [1]. The board comprises a PIC32 microprocessor and a Texas Instruments power stage, and it communicates with a host processor over a serial interface. A position sensor provides rotation odometry

and a Hall effect sensor mounted on the propeller shaft provides a top-dead-center reference for the blade orientation. The derivative of this position feedback provides an instantaneous speed estimate.

To control the thruster, the host sends 4 parameters via the serial connection. These are the force, rudder, and elevator commands, in addition to a direction command that dictates whether to spin clockwise or counterclockwise. Based on the relationships explored in the preceding section, the motor controller adjusts these commands and their output. The motor controller board replies with the same message scheme representative of the measured response of the output shaft.

The motor controller was integrated into a custom designed 3-inch thruster with a magnetically coupled drive shaft between the brushless DC motor and the single-bladed propeller. Inside the housing are batteries, a small computer, an attitude heading reference system (AHRS) and a pressure sensor. The platform can perform simple, pre-scripted missions that either directly control the thruster parameters or command the thruster to maintain a given heading, pitch, or depth.

IV. RESULTS

We tested our asymmetrically propelled platform this past summer in Great Harbor in Woods Hole, Massachusetts. The system performed multiple surface maneuvers, demonstrating the ability to both turn as commanded and to follow a commanded heading. Figure 7 shows a composite of 5 photographs of the platform captured during a turn to port at approximately 3 knots or 1.5 meters per second. This test provided a qualitative assessment that the platform has a turning radius on the order of several body lengths. These values represent typical speeds and turning radii of similarly shaped AUVs executing typical survey missions.

We also tested the platform in a tank with a pre-scripted mission aimed at demonstrating an ability to maneuver in place. It was commanded to first move forward while turning to port and then reverse while turning to port. This process was repeated every second for a period of time. The result was a slow turn while staying in roughly the same location. This maneuver was repeated to starboard as well. For these tests, the platform was ballasted as closely to neutral as possible since it cannot be directly controlled along its vertical z -axis. Figure 8 shows a composite of 7 photographs of the platform captured during a maneuver to port. Alternating forward-port, reverse-port commands induced a port turn of approximately 74° over 24 seconds, while alternating forward-starboard, reverse-starboard commands induced a starboard turn of approximately 60° over 16 seconds. Thus, average turning rates of around 3-4 degrees per second were observed using this approach.

V. DISCUSSION

We have successfully proven the concept of asymmetric propulsion and demonstrated its ability to be harnessed to control the movement of an underwater robot. This technology addresses several key issues in the space of AUV design



Fig. 7. A composite of 5 images showing multiple platform orientations as it executes a turn to port while on the surface.



Fig. 8. A composite of 7 images demonstrating an ability to maneuver in place.

including size, complexity, drag, and maneuverability, all of which contribute significantly to endurance and mission capabilities. It allows vehicles to maintain maneuverability throughout a full range of speeds, and a vehicle utilizing

such a system may be capable of orientating itself at very low speeds without the need for additional thrusters. This type of low-speed maneuverability could enable an AUV to hold station, hover, or enter low-power loiter behaviors. It also has the potential to offer improvements in efficiency, reliability, and cost as compared to existing propulsion and maneuvering systems. Follow-on work will focus on more advanced control schemes and sensor-based feedback to refine this as an enabling capability for AUV missions.

One type of AUV mission this technology would enable is wide-area, over-the-horizon surveys that require high-resolution imagery of several discrete objects. An asymmetric propulsion system would enable the AUV to make a low-speed, energy-efficient transit to the survey site, then increase to the optimal speed for a sonar survey. Upon detecting an interesting object, the AUV could reduce its altitude, maneuvering slowly over the object while capturing high-resolution imagery and stitching together a three-dimensional model. This could also enable autonomous manipulation or recovery of specific objects as well. A single-mission paradigm such as this would dramatically reduce the costs of operations that currently require multiple missions with different classes of robotic vehicles. It could potentially eliminate the need for a surface support ship as well.

Asymmetric propulsion is a key enabling technology that will propel the next generation of marine robots. These platforms will have enhanced autonomous capabilities, extended endurance, and be equipped with novel ways to interact with

their environments. At the same time they must be matched with equally capable hardware and propulsion systems that will maximize the utility of these new developments. We see great utility for asymmetric propulsion, not only as an enabler in high-end AUVs, but also as a simplifying, cost-saving factor in the smaller, inexpensive systems that will ultimately bring AUVs to a broader user base.

ACKNOWLEDGMENT

We would like to thank Tom Austin, Ben Allen, and Mike Purcell for their inspiration and guidance. We would also like to thank David Knaack, Allison Markova, Gabe Hendricks, Anthony Piri, and Rusty Warren for their valuable insight into the applications for this technology.

REFERENCES

- [1] R. H. Littlefield, F. Jaffre, and J. W. Kaeli, "Auv propulsion and maneuvering by means of asymmetric thrust," in *2018 IEEE/OES Autonomous Underwater Vehicle Workshop (AUV)*. IEEE, 2018, pp. 1–6.
- [2] B. Allen, W. S. Vorus, and T. Prestero, "Propulsion system performance enhancements on remus auvs," in *Oceans 2000 MTS/IEEE Conference and Exhibition*, vol. 3. IEEE, 2000, pp. 1869–1873.
- [3] H. Singh, D. Yoerger, and A. Bradley, "Issues in auv design and deployment for oceanographic research," in *Robotics and Automation, 1997. Proceedings., 1997 IEEE International Conference on*, vol. 3. IEEE, 1997, pp. 1857–1862.
- [4] The Voith Group. (2019) Voith schneider propeller. [Online]. Available: <http://voith.com/corp-en/drives-transmissions/voith-schneider-propeller-vsp.html>
- [5] B. K. Rawdon, "Single blade propeller with variable pitch," Feb. 13 2018, uS Patent 9,889,925.
- [6] M. Beretta, P. Balocchi, and G. Fumagalli, "Propeller propulsion unit for aircrafts in general," Oct. 26 1999, uS Patent 5,971,322.
- [7] M. E. Furlong, D. Paxton, P. Stevenson, M. Pebody, S. D. McPhail, and J. Perrett, "Autosub long range: A long range deep diving auv for ocean monitoring," in *2012 IEEE/OES Autonomous Underwater Vehicles (AUV)*. IEEE, 2012, pp. 1–7.
- [8] R. B. Carelli, "Use of an asymmetric propeller for unmanned underwater vehicles," Massachusetts Institute Of Technology Cambridge United States, Tech. Rep., 2019.
- [9] T. Austin, M. Purcell, F. Jaffre, J. Kaeli, B. Allen, and R. Littlefield, "Asymmetric propulsion and maneuvering system," Jan. 23 2018, US Patent 9,873,499.
- [10] D. Yue. (Spring 2005) Marine Hydrodynamics (13.021). <https://ocw.mit.edu>. Massachusetts Institute of Technology: MIT OpenCourseWare.